

## Article

# Target-Based 6-5 Fused Ring Heterocyclic Scaffolds Display Broad Antiparasitic Potency In Vitro

Darline Dize <sup>1</sup>, Mariscal Brice Tchatat Tali <sup>1</sup>, Cyrille Armel Njanpa Ngansop <sup>1</sup>, Rodrigue Keumoe <sup>1</sup>, Eugenie Aimée Madiesse Kemgne <sup>1,2</sup>, Lauve Rachel Tchokouaha Yamthe <sup>1,3</sup>, Patrick Valere Tsouh Fokou <sup>1,4</sup>, Boniface Pone Kamdem <sup>1,\*</sup>, Katsura Hata <sup>5</sup> and Fabrice Fekam Boyom <sup>1,2,\*</sup>

<sup>1</sup> Antimicrobial and Biocontrol Agents Unit (AmBcAU), Department of Biochemistry, Faculty of Science, University of Yaounde I, Yaounde P.O. Box 12558, Cameroon; eugeniefekam@gmail.com (E.A.M.K.)

<sup>2</sup> Advanced Research & Health Innovation Hub, Yaounde P.O. Box 20133, Cameroon

<sup>3</sup> Institute for Medicinal Research and Medicinal Plants Studies, Yaounde P.O. Box 6163, Cameroon

<sup>4</sup> Department of Biochemistry, Faculty of Sciences, University of Bamenda, Bambili P.O. Box 39, Cameroon

<sup>5</sup> Global Health Research Section, hhc Data Creation Center, Eisai Co., Ltd., 1-3, Tokodai 5-chome, Tsukuba-shi 300-2635, Ibaraki, Japan

\* Correspondence: ponekamdemboniface@gmail.com (B.P.K.); boyomf@arhih.cm or fabrice.boyom@fulbrightmail.org (F.F.B.)

**Abstract:** Malaria, leishmaniasis, and African trypanosomiasis are protozoan diseases that constitute major global health problems, especially in developing countries; however, the development of drug resistance coupled with the toxicity of current treatments has hindered their management. The involvement of certain enzymes (dihydrofolate reductase [DHFR]) or proteins (potassium channels) in the pathogenesis of these protozoan diseases is undeniable. In this study, a series of three DHFR inhibitors (6-5 fused heterocyclic derivatives X, Y, and Z) and one K<sup>+</sup> channel blocker (E4031) were screened for their inhibitory effects on *Leishmania donovani*, *Plasmodium falciparum*, and *Trypanosoma brucei*. A resazurin assay was used to assess the antitrypanosomal and antileishmanial activities of the test compounds, whereas the antiplasmodial activity was evaluated through the SYBR Green I test. Moreover, the cytotoxicities of the test compounds were evaluated in Vero, Raw 264.7, and HepG-2 cells using a resazurin-based test, while their pharmacokinetic properties were predicted using the online tool, pkCSM. As a result, compound Y exhibited selective (selectivity index range: from 2.69 to >61.4; Vero, Raw 264.7, and HepG-2 cells) and broad-spectrum antiprotozoal activity against *L. donovani* promastigotes (IC<sub>50</sub>: 12.4 μM), amastigotes (IC<sub>50</sub>: 4.28 μM), *P. falciparum* (IC<sub>50</sub>: 0.028 μM), and *T. brucei brucei* (IC<sub>50</sub>: 0.81 μM). In addition, compound X inhibited the growth of *P. falciparum* (IC<sub>50</sub>: 0.0052 μM) and *T. brucei brucei* (IC<sub>50</sub>: 6.49 μM). In silico screening of the active antiprotozoal compounds revealed positive drug likeness scores, as none of the criteria for Lipinski's rule were violated by these compounds. However, in-depth pharmacokinetic and mechanistic studies are warranted to support the discovery of novel antiprotozoal agents against malaria, leishmaniasis, and African trypanosomiasis by repurposing K<sup>+</sup> channel blockers and DHFR inhibitors.

**Keywords:** protozoan diseases; drug repurposing; cytotoxicity; dihydrofolate reductase inhibitors; potassium (K<sup>+</sup>) channel blocker; ADME properties



**Citation:** Dize, D.; Tali, M.B.T.; Ngansop, C.A.N.; Keumoe, R.; Madiesse Kemgne, E.A.; Yamthe, L.R.T.; Tsouh Fokou, P.V.; Pone Kamdem, B.; Hata, K.; Fekam Boyom, F. Target-Based 6-5 Fused Ring Heterocyclic Scaffolds Display Broad Antiparasitic Potency In Vitro. *Future Pharmacol.* **2024**, *4*, 188–198. <https://doi.org/10.3390/futurepharmacol4010013>

Academic Editors: Fabrizio Schifano and Gabriel Navarrete-Vázquez

Received: 8 January 2024

Revised: 10 February 2024

Accepted: 27 February 2024

Published: 28 February 2024



**Copyright:** © 2024 by the authors. Licensee MDPI, Basel, Switzerland. This article is an open access article distributed under the terms and conditions of the Creative Commons Attribution (CC BY) license (<https://creativecommons.org/licenses/by/4.0/>).

## 1. Introduction

Parasitic diseases represent an overwhelming health problem for impoverished populations living in developing countries with poor sanitary conditions. Previous reports have shown that the three most important protozoan diseases have an estimated disability-adjusted life year (DALY) of approximately one million [1]. These diseases include malaria, leishmaniasis, and trypanosomiasis, which are caused by vector-borne protozoan parasites, including *Plasmodium*, *Leishmania*, and *Trypanosoma* species, respectively. In 2022, the World Health Organization (WHO) documented a total of 249 million cases of malaria

with 608,000 deaths, and with 94% of cases (233 million) and 95% (580,000) of deaths in the African region [2,3]. Core activities for the management of malaria include vector control and treatment of patients with appropriate antimalarial drugs, all of which are impaired by the endless development of mosquito- and *Plasmodium* spp.-resistant strains, and potential vaccine administration [2,4]. In addition, leishmaniasis and trypanosomiasis are neglected tropical diseases (NTDs) that can be fatal if left untreated [5].

Leishmaniasis is endemic in Africa, Asia, the Americas, and the Mediterranean region [6], where it can develop into three main clinical forms according to the involved *Leishmania* species. These include cutaneous and mucocutaneous forms (*Leishmania major*, *L. tropica*, *L. braziliensis*, etc.) and the most severe visceral forms (*L. donovani*, *L. infantum*, etc.) [7]. Annually, 700,000 to 1 million people are newly infected with leishmaniasis, with 20,000 to 30,000 deaths [7]. The treatment options for leishmaniasis include pentavalent antimonials, sodium stibogluconate (pentostam), and meglumine antimoniate (glucantime) as first-line drugs and pentamidine, amphotericin B, paromomycin, and miltefosine as second-line treatments [8].

African trypanosomiasis, which affects both humans (human African trypanosomiasis) and animals (animal African trypanosomiasis), is a health concern in endemic areas. Human African trypanosomiasis (HAT) threatens millions of people in 36 sub-Saharan African countries, with 55 million people at risk of being infected [9]. With the initiation of multiple control strategies, an important decline in the number of new cases from approximately 40,000 in 1998 to 663 in 2020 was recorded. However, important efforts should be made to completely fulfill the WHO's initiative toward the eradication of sleeping sickness by 2030 [9]. *Trypanosoma brucei* gambiense and *T. brucei* rhodesiense are the main pathogens responsible for HATs. Animal African trypanosomiasis (AAT) is among the most common diseases in cattle and has severe economic consequences [10]. Indeed, the disease was reported to cause 3 million deaths in cattle [11]. AAT is caused by three main species of the genus *Trypanosoma*, namely *T. brucei* gambiense, *T. vivax*, and *T. congolense*. Pentamidine, eflornithine, nifurtimox, fexinidazole, suramin, and melarsoprol are among the current treatments for HAT, whereas homidium bromide, diminazene aceturate, and suramin are the main drugs for AAT [9]. However, these drugs exhibit poor efficacy, unacceptable toxicity, and drug resistance, which limit their usefulness [10,12]. The currently developed acoziborole drug, which showed a 95% success rate and effectiveness during phase 2 and 3 trials against HAT, is noteworthy; however, recent developments in *Trypanosoma* resistance to this drug have been identified [13]. Thus, there is a crucial need to search for alternative treatments against *Trypanosoma* infections.

Despite recent advances in research on controlling these infectious diseases, they remain prevalent, supporting the need to identify effective and safe treatments for malaria, leishmaniasis, and trypanosomiasis. The natural origin of antimalarial drugs is undeniable, as quinine and artemisinin are among the foremost examples that were identified from cinchona bark [14] and *Artemisia annua*, respectively [15]. Moreover, the synthesis and structural modification of natural product scaffolds have provided a number of active principles for antileishmanial (miltefosine) [16,17] and antitrypanosomal (fexinidazole) [9,18] drug development. The mechanistic basis of the antiprotozoal action of these active principals revealed the inhibition of a number of enzymes, such as dihydrofolate reductase (a reported target of anticancer drugs [19,20], which are crucial for the survival and virulence of *Plasmodium* [21], *Leishmania*, and *Trypanosoma* [22,23] species. In fact, dihydrofolate reductase aids in the replication of several microorganisms by reducing dihydrofolate to tetrahydrofolate for DNA synthesis [24,25]. Furthermore, the two antimalarial drugs, cycloguanil and pyrimethamine, as well as a codified antimalarial compound (P218), were also found to inhibit the DHFR enzyme [26]. Unlike the other most popular antifolate agents, such as trimethoprim, cycloguanil, and pyrimethamine, which exhibit weak inhibition of *Leishmania major* DHFR, methotrexate inhibits this enzyme (*L. major* DHFR) in the nanomolar range (IC<sub>50</sub>: 5 nM). Whole-cell phenotypic screening of methotrexate against *L. major* revealed an IC<sub>50</sub> value of 0.3 μM, confirming that this compound might exert antileishmanial activity

through DHFR inhibition [27,28]. Recently, Dize et al. revealed the inhibitory potential of MMV675968 derivatives bearing the quinazoline scaffold on *Trypanosoma brucei brucei* DHFR together with their potent antitrypanosomal activity (IC<sub>50</sub> range: 45–60 nM) [29].

Furthermore, the implication of potassium (K<sup>+</sup>) channels in the survival and virulence of these parasites is noteworthy [30–33]. According to previous studies, K<sup>+</sup> channels are integral membrane proteins that are intricately involved in the maintenance of vital parameters, including the cellular membrane potential and cell volume, in malaria parasites [34]. Modern pharmacological studies revealed several antiprotozoal (clofazimine derivatives [35]) and antiplasmodial (quinidine, clotrimazole, haloperidol, charybdotoxin, bicuculline methiodide, tubocurarine chloride, trifluoperazine hydrochloride, and verrucologen; IC<sub>50</sub> values ranging from 0.046 to 187.86 μM; *Plasmodium falciparum* 3D7) [30] potential hit compounds, which were found to inhibit K<sup>+</sup> channels. In addition, the inhibitory effects of glibenclamide [36] and a few halogenated glucose analogs [37] on K<sup>+</sup> channels have been reported in *Leishmania* spp. and *Trypanosoma brucei*, respectively. Thus, it is not unreasonable to speculate that compounds or drugs that inhibit dihydrofolate reductase or K<sup>+</sup> channels can potentially elicit growth inhibition of the malaria, leishmaniasis, and African trypanosomiasis parasites.

Whole-cell phenotypic screening of compounds with known inhibitory effects against validated therapeutic targets is called target-based drug discovery. This approach includes target identification and validation via a number of tests, such as in silico prediction and biochemical and genetic analyses, to identify proteins or enzymes that are crucial for the survival and virulence of parasites [38]. Indeed, target-based drug discovery and drug repositioning can afford potentially active compounds that can serve as scaffolds for drug development, thereby reducing the overall cost and time frame used in the traditional drug discovery process [39]. Therefore, this study aimed to investigate the antiprotozoal activity of a series of three heterocyclic potential DHFR inhibitors (compounds X, Y, and Z) (Figure 1) and one potassium channel blocker (E4031) originally designed for anticancer research and provided by Eisai Co., Ltd. (Figure 1, Table 1) against *Plasmodium*, *Leishmania*, and *Trypanosoma* parasites.

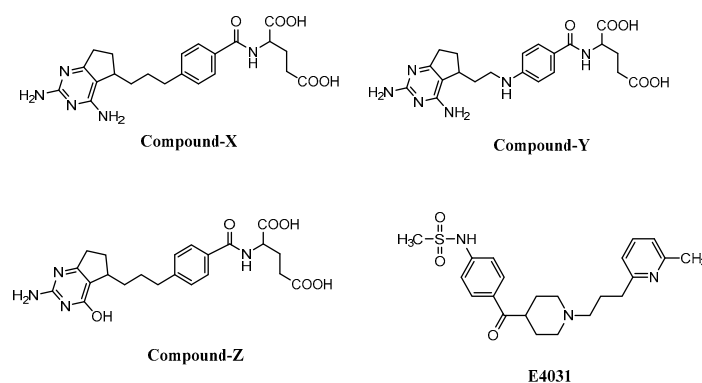


**Figure 1.** Structures of the 6,5-fused ring heterocyclic antifolates (X, Y, Z) and the potassium channel blocker (E4031).

**Table 1.** Reported activities of the various antifolate compounds against DHFR enzymes.

Compounds	* IC <sub>50</sub> (nM)_DHFR			References
	Bovine Liver	P388	CCRF-CEM	
X	2.5	7.1	0.6	[40–42]
Y	5.9	-	0.8	[41,42]
Z	60,000	-	-	[40]

\* Median inhibitory concentration (IC<sub>50</sub>) of the antifolates on DHFR from bovine liver, P388 (leukemia cells), and CCRF-CEM (human T-lymphoblastic leukemia cells).

## 2. Materials and Methods

### 2.1. Parasites and Culture

Three parasites, *P. falciparum* strain 3D7, *L. donovani* 1S (MHOM/SD/62/1S) promastigotes, and *T. brucei* bloodstream trypomastigotes (subsp. *brucei*, Strain Lister 427 VSG 221), which were used in this study, were obtained as kind gifts from the Biodefense and Emerging Infections Research Resources Repository (BEI Resources) (<https://www.beiresources.org/>, accessed on 1 January 2023).

The axenic promastigote forms of *L. donovani* were cultured at 28 °C in M199 culture medium (Sigma Aldrich, St. Louis, MO, USA) supplemented with 1% streptomycin/penicillin (Sigma Aldrich) and 10% heat-inactivated fetal bovine serum (FBS) (Sigma Aldrich).

*Plasmodium falciparum* parasites were continuously maintained in Petri dishes containing complete RPMI 1640 medium [RPMI 1640 (Sigma Aldrich) supplemented with 0.5% Albumax II (Gibco), 0.2% sodium bicarbonate (Sigma Aldrich), 1% hypoxanthine 100X (Gibco), 25 mM HEPES, and 0.04% gentamicin (Sigma Aldrich)] with fresh O+ erythrocytes obtained from healthy human volunteers and suspended in 4% hematocrit (*v/v*), followed by incubation at 37 °C in a 5% CO<sub>2</sub> humidified atmosphere [43]. The culture medium was renewed daily, and parasitemia was monitored via microscopy through 10% Giemsa-stained thin blood smears. Two days prior to the assay, parasites were synchronized at the ring stage via serial treatment with 5% sorbitol.

The bloodstream form of *T. brucei* subsp. *brucei* was grown and maintained in vented flasks containing standard HMI-9 (Hirumi's modified Iscove's medium 9) supplemented with 10% heat-inactivated FBS. Parasites were subsequently incubated at 37 °C in a 5% CO<sub>2</sub> atmosphere and examined by inverted microscopy every 72 h to monitor parasite density. Next, the cells were passaged by transferring 250 µL of the medium containing parasites into 4.750 mL of fresh medium in a new sterile vented flask [44].

### 2.2. Mammalian Cell Line Culture

Three cell lines were used to evaluate the cytotoxicity of the test compounds: the African green monkey kidney cell line (Vero; ATCC CRL-1586), the macrophage murine leukemia cell line (RAW 264.7) (obtained from the American Type Culture Collection (ATCC), Manassas, VA, USA), and the human hepatoma cell line HepG-2 (Acc 85011430) (procured from Sigma Aldrich). Vero and Raw264.7 cells were maintained in T-25 vented cap culture flasks containing complete Dulbecco's modified Eagle medium (DMEM) [10% (*v/v*) heat-inactivated fetal bovine serum (HIFBS), 1% (*v/v*) nonessential amino acid mixture, and 1% penicillin/streptomycin], followed by incubation at 37 °C in a 5% CO<sub>2</sub> humidified atmosphere. Vero and Raw cells were passaged with trypsin-EDTA (ethylenediaminetetraacetic acid) (Gibco, 0.25%) up to approximately 80–90% confluence. HepG-2 cells were grown and maintained in Eagle's minimum essential medium supplemented with 10% (*v/v*) HIFBS, 2.2 g/mL sodium bicarbonate, 1% penicillin/streptomycin, and 1% sodium pyruvate at 37 °C under the same conditions. The cells were passaged every 72 h to maintain a cell density of between  $1 \times 10^5$  and  $3 \times 10^5$  cells/mL in a 25 cm<sup>2</sup> culture flask.

### 2.3. Antiparasitic Assays

#### 2.3.1. Antikinetoplastid Activity

Assays for *Trypanosoma brucei* Bloodstream and *Leishmania donovani* Promastigote Inhibition

A resazurin assay was used to determine the antitrypanosomal and antileishmanial activities of the compounds in a 96-well microplate using modified protocols, as reported by Bowling et al. [45] and Siqueira-Neto et al. [46], respectively. Either  $2 \times 10^5$  trypanosomes or  $4 \times 10^5$  *Leishmania* promastigotes per mL were seeded with various compounds (concentrations ranging from 10 to 0.016 µM). The final concentration of dimethylsulfoxide (DMSO) was kept at 0.1%, and a vehicle control was used in all assays. Pentamidine (1–0.0016 µM) and amphotericin B (10–0.16 µg/mL) were used as positive controls for *Trypanosoma* and *Leishmania*, respectively. After a 24 h incubation of the *Leishmania* plates, 1 mg/mL resazurin dye (prepared in Dulbecco's phosphate-buffered saline) was added, followed by incubation

for 48 h in the dark. Following a 68 h incubation period for trypanosomes at 37 °C and 5% CO<sub>2</sub>, 10 µL of resazurin solution (0.15 mg/mL) was added to each well, and the plates were subsequently incubated for an additional 4 h. For both tests, the fluorescence was then read using a Tecan Infinite F200 reader using excitation and emission wavelengths of 530 and 590 nm, respectively.

#### Antiamastigote Assay

Compounds that displayed activity against the promastigote forms were further screened against the intracellular amastigotes of *L. donovani* as reported by Jain et al. [47] with slight modifications (using Raw 264.7 macrophages as host cells in lieu of THP-1 human acute monocytic leukemia cells). In brief, exponentially growing Raw 264.7 macrophages ( $4 \times 10^3$  cells/well) were seeded in sterile flat-bottomed 96-well plates and then incubated for 6 h at 37 °C under 5% CO<sub>2</sub> to allow adhesion. Next, the plates were washed with sterile PBS to remove nonadherent cells and further incubated for 24 h at 37 °C in a 5% CO<sub>2</sub> atmosphere with M199 medium containing *Leishmania* metacyclic promastigotes ( $4 \times 10^5$  cells) at a 1:10 macrophage/promastigote ratio. Thereafter, 3–4 successive washes with phosphate-buffered saline (PBS) were applied to carefully remove the noninternalized promastigote forms. A solution containing 10% FBS, fresh M199 medium, and test compounds (final assay concentrations ranging from 10 to 0.016 µM) was prepared and incubated for 48 h at 37 °C in a 5% CO<sub>2</sub> atmosphere. Next, 0.05% SDS (sodium dodecyl sulfate) was added to the plates, which were incubated for 30 s for controlled lysis, followed by the addition of complete M199 (10% FBS) to stop macrophage lysis. Afterwards, resazurin (250 µg/mL) was added to each well, followed by incubation for 24 h. Then, the fluorescence of the preparation was read using a microplate reader (TECAN-Infinite M200, Tecan Austria GmbH, Grödig Flachgau, Austria) at λexcitation and λemission wavelengths of 530 and 590 nm, respectively.

#### 2.3.2. Antiplasmodial Assay

The SYBR Green I-based fluorescence method was used to assess the antiplasmodial activity of the selected compounds [48]. Briefly, 10 µL of each compound was added to a 96-well assay plate in duplicate and serially diluted to reach final concentrations ranging from 10 to 0.016 µM. Artemisinin (10 µM) and chloroquine (10 µM) were used as positive controls (0% growth), whereas 0.1% DMSO (*v/v*) was used as a negative control (100% growth). Next, 90 µL of parasitized red blood cells at 1% hematocrit and 2% parasitaemia were dispensed into each well, followed by incubation of the preparation for 72 h. To evaluate parasite growth, the presence or absence of trophozoites was immediately checked in the plates. For this purpose, the cells were lysed by performing freeze–thaw cycles, after which 50 µL of the thawed culture in each well was gently mixed with 50 µL of SYBR Green I lysis buffer [0.2 µL of 10,000×SYBR Green I (Invitrogen, Waltham, MA, USA) per mL of lysis buffer {Tris (20 mM; pH 7.5), saponin (0.008%; *wt/v*), EDTA (5 mM), and Triton X-100 (0.08%; *v/v*)}]. The plates were further incubated for an additional 60 min in darkness at room temperature, after which the fluorescence was measured using a microplate reader (TECAN-Infinite M200, Tecan Austria GmbH, Grödig Flachgau, Austria) at excitation and emission wavelengths of 485 and 530 nm, respectively.

#### 2.4. Cytotoxicity Assay

The resazurin-based colorimetric method [45] was used to assess the cytotoxic effects of the active antiprotozoal compounds against two human mammalian cells, *viz.* Raw 264.7 and Vero cells, as well as human hepatoma HepG-2 cells. In brief, cells were seeded at  $10^4$  cells/well (100 µL) in 96-well culture plates and incubated overnight to allow cell adherence. After the culture medium was renewed, 10 µL of serially diluted compound solution (concentration range: 50–0.08 µM) was added in duplicate. The plates were then incubated at 37 °C for 48 h in a 5% CO<sub>2</sub> humidified atmosphere. Wells containing 10% DMSO (*v/v*) and podophyllotoxin (20 µM) were regarded as positive controls, while those

containing only cultured cells were considered to have 100% growth. Next, ten microliters of a stock solution of resazurin [0.15 mg/mL, Dulbecco's phosphate-buffered saline (DPBS)] was added to each well, gently mixed, and subsequently incubated for an additional 4 h. Fluorescence was read using a microplate reader (TECAN-Infinite M200, Tecan Austria GmbH, Grödig Flachgau, Austria) with excitation and emission wavelengths of 530 and 590 nm, respectively.

### 2.5. *In Silico* Prediction of Physicochemical and Pharmacokinetic Properties

The studied compounds were subjected to *in silico* studies to predict their absorption, distribution, metabolism, and excretion profiles [49]. The chemical structures of the test compounds were drawn using ChemBio2D Draw, whereas their SMILES codes were produced and further used as the main material to predict the pharmacokinetic properties by running the pkCSM online tool (<https://biosig.lab.uq.edu.au/pkcsm/prediction>; accessed on 13 August 2022).

### 2.6. Data Analysis

Each experiment was carried out in duplicate and repeated twice. The growth inhibition percentages for each test compound were determined using Microsoft Excel software (version 2013, Washington, DC, United States of America) and then used for dose—response curve plotting (inhibitory percentage versus log<sub>10</sub> [drug concentration]) to deduce the half-maximal inhibitory concentration (IC<sub>50</sub>) or the half-cytotoxic concentration (CC<sub>50</sub>) using GraphPad Prism 8.0 software. Compound selectivity indices were calculated for each test sample as follows: SI=CC<sub>50</sub> cells/IC<sub>50</sub> parasites.

## 3. Results and Discussion

In this study, the antiprotozoal activities of a series of DHFR inhibitors (compounds X, Y, and Z) and the potassium channel blocker, E4031, were evaluated against *Plasmodium*, *Leishmania*, and *Trypanosoma* species. As a result, compounds X, Y, and Z and E4031 showed different degrees of antiprotozoal activity, ranging from poor (IC<sub>50</sub> > 10 μM) to promising (IC<sub>50</sub> < 10 μM) according to previously reported criteria [50,51].

Against *T. brucei*, compounds X and Y exhibited IC<sub>50</sub> values of 6.49 and 0.81 μM, respectively, compared with pentamidine (IC<sub>50</sub> value: 0.006 μM), whereas these compounds had IC<sub>50</sub> values of 0.0052 and 0.028 μM, respectively, when tested against *Plasmodium falciparum* 3D7, and high parasite selectivity for Raw, Vero, and HepG-2 cells (SI > 366), compared with the values obtained with artemisinin (IC<sub>50</sub>: 0.03 μM) (Table 2).

In addition, the broad-spectrum inhibitor Y had IC<sub>50</sub> values of 12.47 and 4.28 μM when tested against *L. donovani* promastigotes and amastigotes, respectively, with SI ranging from 2.69—>11.7 vs. amphotericin B (IC<sub>50</sub> values: 0.020 and 0.247.81 μM, respectively).

Furthermore, compounds Z and E4031 had less activity when tested against *T. brucei* and *P. falciparum* 3D7 (IC<sub>50</sub> values > 10 μM), and promastigotes of *L. donovani* (IC<sub>50</sub> values = 10 μM) and were predicted to be poorly active compounds. The different levels of selectivity of the inhibitors for the three parasites can be justified based on several factors, including target specificity, genetic variability, structural differences in their essential biomolecules, such as enzymes or receptors, and resistance profile to specific inhibitors due to variations in their resistance mechanisms. The rationale often lies in the unique biochemical, genetic, or structural features that distinguish one parasite from another. Although numerous authors have reported the anticancer and antifolate activities of compounds X, Y, and Z [40,42], the antiprotozoal activity of these compounds has not yet been characterized. In fact, the 6,5-fused heterocyclic systems X, Y, and Z share a number of common features, such as the presence of pyrimidine, amino, and amide groups. According to the literature, there is evidence that 6,5-fused heterocyclic compounds exhibit a wide range of biological activity, including antiprotozoal activity [52,53]. In addition, the involvement of amino [54], amide [55], and pyrimidine [56,57] moieties in potent antiprotozoal hit compounds is indubitable. Thus, pyrimidine, amino, and amide groups embodied in the studied 6,5-fused

heterocyclic compounds (X and Y) might have contributed to the observed antiprotozoal activities. Although X, Y, and Z are structurally similar compounds, one amino group of the pyrimidine moiety is replaced by an OH group in compound Z. This structural modification might have contributed to the decrease in the observed antiprotozoal activity of compound Z, compared to their counterparts X and Y. Even though there is reported evidence that the presence of OH groups tends to increase the antiprotozoal activity of bioactive compounds [58], other reports highlight a different opinion on this matter [59].

The selection of compounds based on their drug-likeness scores increases the likelihood of identifying potential drug candidates with favorable pharmacokinetics, efficacy, and safety. As realigning pharmacokinetic studies early in the discovery phase can assist in selecting an ideal drug candidate, active antiprotozoal compounds were subjected to *in silico* screening using the pkCSM online tool. According to the *in silico* analysis of physicochemical properties, the molecular weight (441.488, 442.472, 442.476, and 415.559), ClogP (lipophilic; octanol–water partition coefficient) (1.741, 1.865, 1.221, and 3.289), rotatable bonds (10, 10, 10, and 8), hydrogen bond acceptors (HBAs) (7, 7, 8, and 5), hydrogen bond donors (HBDs) (5, 5, 6, and 1), and topological polar surface area (TPSA) (184.604, 184.058, 183.789, and 172.949) (Table S1, see Supplementary Material) of compounds X, Y, and Z and E4031 were predicted. Notably, none of these physicochemical parameters were violated according to the criteria of Lipinski's rule of five, which states that a molecule has an increased chance of being directly bioavailable when it obeys the conditions of having (i) no more than five hydrogen bond donors, (ii) ten hydrogen bond acceptors, (iii) a molecular weight of less than 500, or (iv) a LogP value of less than 5 [60]. In fact, all the tested compounds (X, Y, Z, and E4031) qualify as orally active compounds because they abide by "Lipinski's rule of five" criteria [61,62]. Other rulesets for drug-likeness, including the Veber [flexibility (rotatable bonds):  $< 10$ ; HBD  $\leq 5$ ; HBA  $\leq 10$ ; except for TPSA (140 Å<sup>2</sup>)], Ghose filter ( $-0.4 < \text{Log P} < +5.6$ ; HBD  $\leq 5$  and HBA  $\leq 10$ ; MW  $< 500$  g/mol), Muegge (HBD  $\leq 5$ , except for E4031 and MW  $< 500$  g/mol), and Egan ( $-0.4 < \text{Log P} < +5.6$ ; MW  $< 500$  g/mol and HBA  $\leq 10$ ) rules, showed favorable drug-like characteristics [61,62]. Furthermore, *in silico* tests of ADME (absorption, distribution, metabolism, and excretion) revealed poor permeability of compounds X, Y, and Z and E4031 across the skin, blood–brain barrier, and central nervous system. Nevertheless, *in vitro* and *in vivo* pharmacokinetic studies need to be performed to determine the successful utilization of these compounds as scaffolds in antiprotozoal drug discovery.

We report that a series of three DHFR inhibitors (6-5 fused ring heterocyclic derivatives) and a K<sup>+</sup> channel blocker (E4031) exhibit antiprotozoal activity against three parasite strains, namely *Leishmania donovani*, *Trypanosoma brucei*, and *Plasmodium falciparum* 3D7, without cytotoxicity to the human mammalian cells, Vero or Raw, as well as HepG-2 cells. *In silico* screening of the active antiprotozoal compounds using the pkCSM online tool revealed positive drug-likeness scores, as none of the physicochemical parameters of these compounds violated the criteria of Lipinski's rule of five. Nonetheless, in-depth *in vitro* and *in vivo* pharmacokinetic and antiprotozoal mechanistic studies are warranted to support the discovery of novel antiprotozoal agents against malaria, leishmaniasis, and African trypanosomiasis by repurposing the 6-5 fused ring heterocyclic DHFR inhibitors, while combining structural biology, bioinformatics, medicinal chemistry, and pharmacology tools.

**Table 2.** Antiparasitic and cytotoxic activities of the 6,5-fused ring heterocyclic antifolates and the potassium channel blocker.

Compounds ID	IC <sub>50</sub> ± SD (μM)						CC <sub>50</sub> ± SD (μM)						SI																			
	<i>T. b. brucei</i>		<i>L. donovani Prom</i>		<i>L. donovani ama</i>		<i>Pf_3D7</i>		Raw264.7		Vero		HepG-2		<i>T. b. brucei</i>		<i>L. donovani prom</i>		<i>L. donovani ama</i>		<i>Pf_3D7</i>											
	IC <sub>50</sub>	SD	IC <sub>50</sub>	SD	IC <sub>50</sub>	SD	IC <sub>50</sub>	SD	IC <sub>50</sub>	SD	IC <sub>50</sub>	SD	IC <sub>50</sub>	SD	IC <sub>50</sub>	SD	IC <sub>50</sub>	SD	IC <sub>50</sub>	SD	IC <sub>50</sub>	SD	IC <sub>50</sub>	SD								
Compound-X	6.49 ± 0.4		<10		NT		0.0052		1.91 ± 0.09		<50		<50		<50		0.29		<7.7		2.69		<4		7.85		<11.7		366.6		<9596	
Compound-Y	0.81 ± 0.00		12.47 ± 3.04		4.28 ± 0.12		0.028		33.58 ± 5.5		<50		<50		<50		41		<61.4		2.69		<4		7.85		<11.7		1179		<1756	
Compound-Z	<10		<10		NT		<10		<50		<50		<50		<50						<5											
E4031	<10		10		NT		<10		<50		<50		<50		<50						<5											
Pentamidine	0.006 ± 0.00								>50		>50		>50		>50		>8000		>8000													
Artemisinin							0.03 ± 0.004		>50		>50		>50		>50													>1600		>1600		
Amphotericin B			0.020 ± 0.0016		0.248 ± 0.024				>50		>50		>50		>50						>2500		>2500		>201		>201					

Ama: amastigoste. IC<sub>50</sub>: half-maximal inhibitory concentrations were calculated from two replicates of *P. falciparum*, *T. brucei brucei*, *L. donovani* promastigotes, and intracellular amastigotes. CC<sub>50</sub>: half-maximal cytotoxic concentration in Vero, Raw 264.7, and HepG-2 cells. Prom: promastigote. SI: selectivity index. The positive controls used were amphotericin B for *L. donovani*, pentamidine for *T. brucei brucei*, and artemisinin for *P. falciparum*.

**Supplementary Materials:** The following supporting information can be downloaded at: <https://www.mdpi.com/article/10.3390/futurepharmacol4010013/s1>, Table S1: Predicted physicochemical and ADME properties of the test compounds.

**Author Contributions:** Conceptualization, F.F.B.; methodology, D.D., M.B.T.T., C.A.N.N., K.H. and R.K.; software, D.D., M.B.T.T., C.A.N.N. and R.K.; validation, E.A.M.K., L.R.T.Y., B.P.K., P.V.T.F. and F.F.B.; formal analysis, K.H., B.P.K., E.A.M.K., L.R.T.Y. and P.V.T.F.; investigation, K.H., D.D., M.B.T.T., C.A.N.N. and R.K.; resources, B.P.K., E.A.M.K., L.R.T.Y., P.V.T.F. and F.F.B.; data curation, D.D., M.B.T.T., C.A.N.N. and R.K.; writing—original draft preparation, D.D., M.B.T.T., C.A.N.N., E.A.M.K., L.R.T.Y., K.H. and R.K.; writing—review and editing, E.A.M.K., L.R.T.Y., P.V.T.F., B.P.K. and F.F.B.; visualization, E.A.M.K., L.R.T.Y., P.V.T.F. and B.P.K.; supervision, F.F.B.; project administration, F.F.B.; funding acquisition, F.F.B. All authors have read and agreed to the published version of the manuscript.

**Funding:** This research was funded by the Grand Challenges Africa programme [GCA/DD/rnd3/006], which was awarded to FFB. The Grand Challenges Africa, which is an AAS (African Academy of Sciences) programme, was implemented through the Alliance for Accelerating Excellence in Science in Africa (AESA) platform, an initiative of AAS and the African Union Development Agency-New Partnership for Africa's Development (AUDA-NEPAD). For this work, GC Africa's support was also empowered by the Bill & Melinda Gates Foundation (BMGF), Medicines for Malaria Venture (MMV), and Drug Discovery and Development Centre of University of Cape Town (H3D), and the APC was funded by the authors.

**Institutional Review Board Statement:** Not applicable.

**Informed Consent Statement:** Not applicable.

**Data Availability Statement:** Data are contained within the article and Supplementary Material.

**Acknowledgments:** The authors acknowledge Eisai Co., Ltd., for supporting, designing, and supplying the 6-5 fused ring heterocyclic antifolates (Compound-X, Compound-Y, and Compound-Z) and the potassium channel blocker (E4031).

**Conflicts of Interest:** The funding sponsors had no role in the design of the study; in the collection, analyses, or interpretation of data; in the writing of the manuscript, and in the decision to publish the results.

## References

1. Murray, C.J.L.; Vos, T.; Lozano, R.; Naghavi, M.; Flaxman, A.D.; Michaud, C.; Ezzati, M.; Shibuya, K.; Salomon, J.A.; Abdalla, S.; et al. Disability-adjusted life years (DALYs) for 291 diseases and injuries in 21 regions, 1990–2010: A systematic analysis for the Global Burden of Disease Study 2010. *Lancet* **2012**, *380*, 2197–2223. [CrossRef] [PubMed]
2. The World Health Organization (WHO). Malaria. 2023. Available online: <https://www.who.int/news-room/fact-sheets/detail/malaria> (accessed on 15 December 2023).
3. The World Health Organization (WHO). World Malaria Report 2022. 2022. Available online: <https://www.who.int/teams/global-malaria-programme/reports/world-malaria-report-2022> (accessed on 15 December 2023).
4. The World Health Organization (WHO). WHO Recommends Groundbreaking Malaria Vaccine for Children at Risk. 2021. Available online: <https://www.who.int/news/item/06-10-2021-who-recommends-groundbreaking-malaria-vaccine-for-children-at-risk> (accessed on 18 December 2023).
5. The World Health Organization (WHO). First WHO Report on Neglected Tropical Diseases: Working to Overcome the Global Impact of Neglected Tropical Diseases. 2010. Available online: <https://www.who.int/publications/i/item/9789241564090> (accessed on 20 December 2023).
6. Torres-Guerrero, E.; Quintanilla-Cedillo, M.R.; Ruiz-Esmenjaud, J.; Arenas, R. Leishmaniasis: A review. *F1000 Res.* **2017**, *6*, 750. [CrossRef]
7. The World Health Organization (WHO). Leishmaniasis. 2023. Available online: <https://www.who.int/news-room/fact-sheets/detail/leishmaniasis> (accessed on 21 December 2023).
8. Silva-Jardim, I.; Thiemann, O.H.; Anibal, F.F. Leishmaniasis and Chagas disease chemotherapy: A critical review. *J. Braz. Chem. Soc.* **2014**, *25*, 1810–1823. [CrossRef]
9. The World Health Organization (WHO). Trypanosomiasis (Sleeping Sickness). 2023. Available online: <https://www.who.int/news-room/fact-sheets/detail/trypanosomiasis-human-african-sleeping-sickness> (accessed on 21 December 2023).
10. Giordani, F.; Morrison, L.J.; Rowan, T.G.; De Koning, H.P.; Barrett, M.P. The animal trypanosomiasis and their chemotherapy: A review. *Parasitology* **2016**, *143*, 1862–1889. [CrossRef]
11. Food and Agriculture Organization (FAO). Programme Against Africa, Trypanosomiasis. 2023. Available online: <https://www.fao.org/maat/the-programme/the-disease/en/> (accessed on 22 December 2023).
12. Fairlamb, A.H. Chemotherapy of human African trypanosomiasis: Current and future prospects. *Trends Parasitol.* **2003**, *19*, 488–494. [CrossRef] [PubMed]

13. Betu Kumeso, V.K.; Kalonji, W.M.; Rembry, S.; Mordt, O.V.; Tete, D.N.; Prêtre, A.; Delhomme, S.; Kyhi, M.I.W.; Camara, M.; Catusse, J.; et al. Efficacy and safety of acoziborole in patients with human African trypanosomiasis caused by *Trypanosoma brucei* gambiense: A multicenter, open-label, single-arm, phase 2/3 trial. *Lancet Infect. Dis.* **2023**, *23*, 463–470. [[CrossRef](#)]
14. Christensen, S.B. Natural products that changed society. *Biomedicines* **2021**, *9*, 472. [[CrossRef](#)]
15. Ma, N.; Zhang, Z.; Liao, F.; Jiang, T.; Tu, Y. The birth of artemisinin. *Pharmacol. Ther.* **2020**, *216*, 107658. [[CrossRef](#)] [[PubMed](#)]
16. Dorlo, T.P.C.; Balasegaram, M.; Beijnen, J.H.; de Vries, P.J. Miltefosine: A review of its pharmacology and therapeutic efficacy in the treatment of leishmaniasis. *J. Antimicrob. Chemother.* **2012**, *67*, 2576–2597. [[CrossRef](#)]
17. Pinto-Martinez, A.K.; Rodriguez-Durán, J.; Serrano-Martin, X.; Hernandez-Rodriguez, V.; Benaim, G. Mechanism of action of miltefosine on *Leishmania donovani* involves the impairment of acidocalcisome function and the activation of the sphingosine-dependent plasma membrane Ca<sup>2+</sup> channel. *Antimicrob. Agents Chemother.* **2017**, *62*, e01614-17. [[CrossRef](#)]
18. Torreele, E.; Bourdin Trunz, B.; Tweats, D.; Kaiser, M.; Brun, R.; Mazué, G.; Bray, M.A.; Pécou, B. Fexinidazole—a new oral nitroimidazole drug candidate entering clinical development for the treatment of sleeping sickness. *PLoS Negl. Trop. Dis.* **2010**, *4*, e923. [[CrossRef](#)]
19. Raimondi, M.V.; Randazzo, O.; La Franca, M.; Barone, G.; Vignoni, E.; Rossi, D.; Collina, S. DHFR inhibitors: Reading the past for discovering novel anticancer agents. *Molecules* **2019**, *24*, 1140. [[CrossRef](#)]
20. Wróbel, A.; Drozdowska, D. Recent design and structure-activity relationship studies on the modifications of DHFR inhibitors as anticancer agents. *Curr. Med. Chem.* **2021**, *28*, 910–939. [[CrossRef](#)]
21. Bilsland, E.; van Vliet, L.; Williams, K.; Feltham, J.; Carrasco, M.P.; Fotoran, W.L.; Cubillos, E.F.G.; Wunderlich, G.; Grötl, M.; Hollfelder, F.; et al. *Plasmodium* dihydrofolate reductase is a second enzyme target for the antimalarial action of triclosan. *Sci. Rep.* **2018**, *8*, 1038. [[CrossRef](#)]
22. Shamshad, H.; Bakri, R.; Mirza, A.Z. Dihydrofolate reductase, thymidylate synthase, and serine hydroxy methyltransferase: Successful targets against some infectious diseases. *Mol. Biol. Rep.* **2022**, *49*, 6659–6691. [[CrossRef](#)]
23. Gangjee, A.; Kurup, S.; Namjoshi, O. Dihydrofolate reductase as a target for chemotherapy in parasites. *Curr. Pharm. Des.* **2007**, *13*, 609–639. [[CrossRef](#)] [[PubMed](#)]
24. Sharma, M.; Chauhan, M. Dihydrofolate reductase as a therapeutic target for infectious diseases: Opportunities and challenges. *Future Med. Chem.* **2012**, *4*, 1335–1365. [[CrossRef](#)]
25. Choudhury, A.A.K.; Vinayagam, S.; Adhikari, N.; Ghosh, S.K.; Sattu, K. Microwave synthesis and antimalarial screening of novel 4-amino benzoic acid (PABA)-substituted pyrimidine derivatives as *Plasmodium falciparum* dihydrofolate reductase inhibitors. *3 Biotech* **2022**, *12*, 170. [[CrossRef](#)]
26. Yuthavong, Y.; Tarnchompoo, B.; Vilaivan, T.; Chitnumsub, P.; Kamchonwongpaisan, S.; Charman, S.A.; McLennan, D.N.; White, K.L.; Vivas, L.; Bongard, E.; et al. Malarial dihydrofolate reductase as a paradigm for drug development against a resistance-compromised target. *Proc. Natl. Acad. Sci. USA* **2012**, *109*, 16823–16828. [[CrossRef](#)] [[PubMed](#)]
27. Gilbert, I.H. Inhibitors of dihydrofolate reductase in leishmania and trypanosomes. *Biochim. Biophys. Acta Mol. Basis Dis.* **2002**, *1587*, 249–257. [[CrossRef](#)] [[PubMed](#)]
28. Teixeira, B.V.F.; Teles, A.L.B.; Silva, S.G.D.; Brito, C.C.B.; Freitas, H.F.; Pires, A.B.L.; Froes, T.Q.; Castilho, M.S. Dual and selective inhibitors of pteridine reductase 1 (PTR1) and dihydrofolate reductase-thymidylate synthase (DHFR-TS) from *Leishmania chagasi*. *J. Enzyme Inhib. Med. Chem.* **2019**, *34*, 1439–1450. [[CrossRef](#)] [[PubMed](#)]
29. Dize, D.; Tata, R.B.; Keumoe, R.; Kouipou Toghueo, R.M.; Tchatat, M.B.; Njanpa, C.N.; Tchuengua, V.C.; Yamthe, L.T.; Fokou, P.V.T.; Laleu, B.; et al. Preliminary structure–activity relationship study of the MMV pathogen box compound MMV675968 (2,4-diaminoquinazoline) unveils novel inhibitors of *Trypanosoma brucei brucei*. *Molecules* **2022**, *27*, 6574. [[CrossRef](#)] [[PubMed](#)]
30. Waller, K.L.; Kim, K.; McDonald, T.V. *Plasmodium falciparum*: Growth response to potassium channel blocking compounds. *Exp. Parasitol.* **2008**, *120*, 280–285. [[CrossRef](#)] [[PubMed](#)]
31. Mosimann, M.; Goshima, S.; Wenzler, T.; Lu, A.; Uozumi, N.; Ma, P. A Trk/HKT-Type K<sup>+</sup> transporter from *Trypanosoma brucei*. *Eukaryot. Cell.* **2010**, *9*, 539–546. [[CrossRef](#)] [[PubMed](#)]
32. Kuang, Q.; Purhonen, P.; Hebert, H. Structure of potassium channels. *Cell. Mol. Life Sci.* **2015**, *72*, 3677–3693. [[CrossRef](#)]
33. Paul, A.; Mubashra, Singh, S. Identification of a novel calcium activated potassium channel from *Leishmania donovani* and in silico predictions of its antigenic features. *Acta Trop.* **2021**, *220*, 105922. [[CrossRef](#)] [[PubMed](#)]
34. Ellekvist, P.; Mlambo, G.; Kumar, N.; Klaerke, D.A. Functional characterization of malaria parasites deficient in the K<sup>+</sup> channel Kch2. *Biochem. Biophys. Res. Commun.* **2017**, *493*, 690–696. [[CrossRef](#)]
35. Barteselli, A.; Casagrande, M.; Basilico, N.; Parapini, S.; Rusconi, C.M.; Tonelli, M.; Boido, V.; Taramelli, D.; Sparatore, F.; Sparatore, A. Clofazimine analogs with antileishmanial and antiplasmodial activity. *Bioorg. Med. Chem.* **2015**, *23*, 55–65. [[CrossRef](#)]
36. Serrano-Martín, X.; Payares, G.; Mendoza-León, A. Glibenclamide, a blocker of K<sup>+</sup>(ATP) channels, shows antileishmanial activity in experimental murine cutaneous leishmaniasis. *Antimicrob. Agents Chemother.* **2006**, *50*, 4214–4216. [[CrossRef](#)]
37. Schmidt, R.S.; Macedo, J.P.; Steinmann, M.E.; Salgado, A.G.; Butikofer, P.; Sigel, E.; Rentsch, D.; Maser, P. Transporters of *Trypanosoma brucei*-phylogeny, physiology, pharmacology. *FEBS J.* **2018**, *285*, 1012–1023. [[CrossRef](#)]
38. Andrade, E.L.; Bento, A.F.; Cavalli, J.; Oliveira, S.K.; Freitas, C.S.; Marcon, R.; Schwanke, R.C.; Siqueira, J.M.; Calixto, J.B. Nonclinical studies required for new drug development—Part I: Early in silico and in vitro studies, new target discovery and validation, proof of principles and robustness of animal studies. *Braz. J. Med. Biol. Res.* **2016**, *49*, e5644. [[CrossRef](#)]

39. Müller, J.; Hemphill, A. Drug target identification in protozoan parasites Drug target identification in protozoan parasites. *Expert Opin. Drug Discov.* **2016**, *11*, 815–824. [[CrossRef](#)]
40. Kotake, Y.; Iijima, A.; Yoshimatau, K.; Tamai, N.; Ozawa, Y.; Koyanagi, N.; Kitoh, K.; Nomura, H. Synthesis and antitumor activities of novel 6-5 fused ring heterocycle antifolates: N-[4-[o-(2-amino-4-substituted-6,7-dihydrocyclopenta[*h*]-pyrimidin-5-yl)alkyl]benzoyl]-L-glutamic Acids. *J. Med. Chem.* **1994**, *37*, 1616–1624. [[CrossRef](#)]
41. Kotake, Y.; Okauchi, T.; Iuima, A.; Yoshimatau, K.; Nomura, H. Novel 6-5 fused ring heterocycle antifolates with potent antitumor activity: Bridge modifications and heterocyclic Benzoyl isosters of 2,4-diamino-6,7-dihydro-5H-cyclopenta[*d*]pyrimidine antifolate. *Chem. Pharm. Bull.* **1995**, *43*, 829–841. [[CrossRef](#)] [[PubMed](#)]
42. Mcguire, J.J.; Bergoltz, V.V.; Heitzman, K.J.; Haile, W.H.; Russell, C.A.; Bolanowska, E. Novel 6,5-fused ring heterocyclic antifolates: Biochemical and biological characterization. *Cancer Res.* **1994**, *54*, 2673–2680. [[PubMed](#)]
43. Trager, W.; Jensen, J.B. Human malaria parasites in continuous culture. *Science* **1976**, *193*, 673–675. [[CrossRef](#)] [[PubMed](#)]
44. Hirumi, H.; Hirumi, K. Continuous cultivation of *Trypanosoma brucei* blood stream forms in a medium containing a low concentration of serum protein without feeder cell layers. *J. Parasitol.* **1989**, *75*, 985–989. [[CrossRef](#)] [[PubMed](#)]
45. Bowling, T.; Mercer, L.; Don, R.; Jacobs, R.; Nare, B. Application of a resazurin-based high-throughput screening assay for the identification and progression of new treatments for human african trypanosomiasis. *Int. J. Parasitol. Drugs Drug Resist.* **2012**, *2*, 262–270. [[CrossRef](#)] [[PubMed](#)]
46. Siqueira-Neto, J.L.; Song, O.R.; Oh, H.; Sohn, J.H.; Yang, G.; Nam, J.; Jang, J.; Cechetto, J.; Lee, C.B.; Moon, S.; et al. Antileishmanial high-throughput drug screening reveals drug candidates with new scaffolds. *PLoS Negl. Trop. Dis.* **2010**, *4*, e675. [[CrossRef](#)] [[PubMed](#)]
47. Jain, S.K.; Sahu, R.; Walker, L.A.; Tekwani, B.L. A parasite rescue and transformation assay for antileishmanial screening against intracellular *Leishmania donovani* amastigotes in THP1 human acute monocytic leukemia cell line. *J. Vis. Exp.* **2012**, *70*, 4054.
48. Smilkstein, M.; Sriwilajaroen, N.; Kelly, J.X.; Wilairat, P.; Riscoe, M. Simple and inexpensive fluorescence-based technique for high-throughput antimalarial drug screening. *Antimicrob. Agents Chemother.* **2004**, *48*, 1803–1806. [[CrossRef](#)]
49. Pires, D.E.V.; Blundell, T.L.; Ascher, D.B. pkCSM: Predicting small-molecule pharmacokinetic and toxicity properties using graph-based signatures. *J. Med. Chem.* **2015**, *58*, 4066–4072. [[CrossRef](#)]
50. Boniface, P.K.; Ferreira, E.I. Flavonoids as efficient scaffolds: Recent trends for malaria, leishmaniasis, Chagas disease, and dengue. *Phytother. Res.* **2019**, *33*, 2473–2517. [[CrossRef](#)]
51. Tchatat Tali, M.B.; Boniface, P.K.; Jean Claude, T.; Fabrice, F.F. Current developments on the antimalarial, antileishmanial, and antitrypanosomal potential and mechanisms of action of *Terminalia* spp. *S. Afr. J. Bot.* **2023**, *156*, 309–333. [[CrossRef](#)]
52. Jacobs, L.; de Kock, C.; Taylor, D.; Pelly, S.C.; Blackie, M.A.L. Synthesis of five libraries of 6,5-fused heterocycles to establish the importance of the heterocyclic core for antiplasmodial activity. *Bioorg. Med. Chem.* **2018**, *26*, 5730–5741. [[CrossRef](#)]
53. Faarasse, S.; El Brahmī, N.; Guillaumet, G.; El Kazzouli, S. Regioselective C-H Functionalization of the six-membered ring of the 6,5-fused heterocyclic systems: An overview. *Molecules* **2021**, *26*, 5763. [[CrossRef](#)]
54. Kurniaty, N.; Maharani, R.; Hidayat, A.T.; Supratman, U. An Overview on antimalarial peptides: Natural sources, synthetic methodology and biological properties. *Molecules* **2023**, *28*, 7778. [[CrossRef](#)]
55. Varela, M.T.; Amaral, M.; Romanelli, M.M.; de Castro Levatti, E.V.; Tempone, A.G.; Fernandes, J.P.S. Optimization of physicochemical properties is a strategy to improve drug-likeness associated with activity: Novel active and selective compounds against *Trypanosoma cruzi*. *Eur. J. Pharm. Sci.* **2022**, *171*, 106114. [[CrossRef](#)] [[PubMed](#)]
56. Kumar, S.; Narasimhan, B. Therapeutic potential of heterocyclic pyrimidine scaffolds. *Chem. Cent. J.* **2018**, *12*, 38. [[CrossRef](#)] [[PubMed](#)]
57. Silva, D.G.; Junker, A.; de Melo, S.M.G.; Fumagalli, F.; Gillespie, J.R.; Molasky, N.; Buckner, F.S.; Matheussen, A.; Caljon, G.; Maes, L.; et al. Synthesis and structure-activity relationships of imidazopyridine/pyrimidine- and furopyridine-based anti-infective agents against trypanosomiasis. *ChemMedChem* **2021**, *16*, 966–975. [[CrossRef](#)]
58. Pérez-Silanes, S.; Berrade, L.; García-Sánchez, R.N.; Mendoza, A.; Galiano, S.; Pérez-Solórzano, B.M.; Nogal-Ruiz, J.J.; Martínez-Fernández, A.R.; Aldana, I.; Monge, A. New 1-aryl-3-substituted propanol derivatives as antimalarial agents. *Molecules* **2009**, *14*, 4120–4135. [[CrossRef](#)] [[PubMed](#)]
59. Ravindar, L.; Hasbullah, S.A.; Rakesh, K.P.; Hassan, N.I. Recent developments in antimalarial activities of 4-aminoquinoline derivatives. *Eur. J. Med. Chem.* **2023**, *256*, 115458. [[CrossRef](#)]
60. Chen, X.; Li, H.; Tian, L.; Li, Q.; Luo, J.; Zhang, Y. Analysis of the physicochemical properties of Acaricides based on Lipinski's Rule of five. *J. Comput. Biol.* **2020**, *27*, 1397–1406. [[CrossRef](#)] [[PubMed](#)]
61. Rai, M.; Singh, A.V.; Paudel, N.; Kanase, A.; Falletta, E.; Kerkar, P.; Heyda, J.; Barghash, R.F.; Pratap Singh, S.; Soos, M. Herbal concoction unveiled: A computational analysis of phytochemicals' pharmacokinetic and toxicological profiles using novel approach methodologies (NAMs). *Curr. Res. Toxicol.* **2023**, *5*, 100118. [[CrossRef](#)] [[PubMed](#)]
62. Guenfoud, F.; Khaoua, O.; Cherak, Z.; Loucif, L.; Boussebaa, W.; Benbellat, N.; Laabassi, M.; Mosset, P. Synthesis, antimicrobial, DFT, and in silico pharmacokinetic profiling of nitroaldol quinoline derivatives: A comprehensive exploration for designing potential oral antibacterial agents targeting DNA-gyrase. *J. Mol. Struct.* **2024**, *1300*, 137293. [[CrossRef](#)]

**Disclaimer/Publisher's Note:** The statements, opinions and data contained in all publications are solely those of the individual author(s) and contributor(s) and not of MDPI and/or the editor(s). MDPI and/or the editor(s) disclaim responsibility for any injury to people or property resulting from any ideas, methods, instructions or products referred to in the content.